

1    **Subduction and Modification Patterns at Middle Part of the**  
2    **Solonker-Xar Moron-Changchun-Yanji Suture: Revealed by Deep**  
3    **Seismic Reflection Profile**

4    **Wei Fu<sup>a</sup>, Hesheng Hou<sup>a,\*</sup>, Rui Gao<sup>b,c</sup>, Jianbo Zhou<sup>d</sup>, Xingzhou Zhang<sup>d</sup>, Lei**  
5                                    **Guo<sup>c</sup>, Rui Guo<sup>a</sup>, Zongdong Pan<sup>a</sup>**

6    a. Chinese Academy of Geological Sciences, Beijing, 100037, China

7    b. School of Earth Science and Engineering, Sun Yat-Sen University, Guangzhou 510275, China

8    c. Institute of Geology, Chinese Academy of Geological Science, Beijing, 100037, China

9    d. College of Earth Science, Jilin University, Changchun, 130000

10  
11    \* Corresponding author; E-mail address: hesheng.hou@126.com

12  
13    **Abstract** In order to study the subduction and modification patterns beneath the  
14    middle part of the Solonker-Xar Moron-Changchun-Yanji Suture, a 160-km-long deep  
15    seismic reflection profile was conducted from Naiman to Ar Horqin Banner, Inner  
16    Mongolia. As a result, the profile presents the reflection characteristics of  
17    "longitudinal stratification and transverse partitioning", the most distinguished  
18    features are large area of south dipping reflections along with a set of "crocodile-like  
19    reflection" identified beneath the middle part of the profile, which are considered to  
20    be key seismological evidences for the stages of southward oceanic subduction and  
21    continental collision occurred between the Songliao-Xilinhhot Massif and the North  
22    China Craton. The former had a width of dozens of kilometers but the latter had a  
23    much smaller scale, which may represent the unique characteristic of "soft collision  
24    orogeny" in NE China. Meanwhile, some reflection patterns are identified to represent  
25    the extensional structures formed after the closure of the ancient ocean, such as

reflections from Mesozoic sediments and faults, as well as the relatively flat reflection Moho which cuts off the oblique reflections from lower crust. Some blank reflections and near horizontal strong reflection clusters in the crust are also identified, which may be the reaction of magmatic activities after the blocks were assembled. This study provides a new perspective for revealing the pattern of continental proliferative orogeny and superimposed reconstruction in the eastern part of the Central Asian Orogenic Belt, as well as discussing the structural background of large area magmatic activities in this area.

**Keywords** Solonker-Xar Moron-Changchun-Yanji Suture; Songliao-Xilinhote Massif; Deep seismic reflection; Subduction

## 1.Introduction

The NE China, located in the east of the Central Asian Orogenic Belt ([Şengör and Natal'in, 1996](#)), not only experienced the convergence of microcontinental blocks during the closure of the Paleo-Asian Ocean ([Liu et al, 2017; Wilde, 2015](#)), but also experienced the superimposed reconstruction of the Mongolian-Okhotsk tectonic domain and the Paleo-Pacific tectonic domain ([Wang et al, 2015; Zhou et al., 2018](#)). The area is mainly covered by a small amount of Precambrian rock mass and a part of late Paleozoic, large area of Mesozoic magmatic rocks and Meso-Cenozoic basin ([Wu et al., 2011;Zhang et al., 2015](#)), is a natural laboratory for studying the mechanism of Phanerozoic continental hyperplasia and post-superposition transformation. The Solonker-Xar Moron-Changchun-Yanji Suture in the south is regarded as the collision boundary of North China Craton and the amalgamated blocks in the NE China, and represents the final closure of the Paleo Asian Ocean ([Jian et al., 2010; Liu et al., 2017; Eizenhöfer and Zhao, 2014](#)).

Predecessors have vaguely referred this suture and the Heihe-Hegenshan Suture to the north (called Eieg Miao-Xilinhote-Heihe Suture by [Xu Bei et al., 2015](#)) as Solonker suture zone ([Eizenhofer and Zhao, 2018](#)) to discuss the eventually closure pattern of the Paleo Asian Ocean. Based on the distribution of arcs and accretionary complexes from Solonker to Hegenshan, it is believed that the final closure of the Paleo Asian Ocean experienced a process of bidirectional subduction ([Xiao et al., 2003](#)), while the suture extending eastward along the Xar Moron to Changchun is the southern belt of the extended Solonker Suture. Abundant geological outcrops, paleomagnetism and geophysics evidence ([Liu et al., 2019](#); [Zhang et al., 2014](#)) basically confirmed west part from Solonker Mountain extends eastward to Linxi area and the eastern section from Changchun to Yanji area ([Li, 2006](#); [Zhou et al., 2018](#)) exist an ancient oceanic closure structure and its closure time is limited. However, the middle part of the suture is covered by the Songliao Basin, which caused a lack of outcrops such as ophiolites. Meanwhile, it was strongly modified by the large left strike-slip faults ([Han et al., 2012](#)) and large area of magmatic activity ([Wu et al., 2011](#)) caused by the subduction of the ancient Pacific Ocean. Rough identification of the suture based on some oil drilling drilled into the basement ([Pei et al., 2007](#)) and some low-precision geophysical data ([Yuan et al., 2015](#)), are not very sufficient to make the division of tectonic units specific. Whether the suture zone really existed in this area, and how did the ancient oceans closed, as well as how the Mesozoic structures was superimposed have always been important issues in the geotectonic study of northeast China.

Deep seismic reflection can provide the most detailed image constraints for studying the deep structure of lithosphere ([Brown et al., 1996](#); [Gao et al., 2016](#)). [Zhang et al. \(2014a\)](#) and [Hou et al. \(2015\)](#) discussed the deep structure of west part of the

Solonker Suture and its northern branch (Heihe-Hegenshan Suture). However, the properties of the southern branch, namely the Xar Moron-Changchun-Yanji Suture, is still lacking the constraints of deep tectonic images. As a result, the Chinese Academy of Geological Sciences laid out a deep seismic reflection profile in the southwest margin of the Songliao Basin in 2016 with full coverage spanning of about 160 km (fig. 1, fig. 2). Based on fine processing of the original data, we made a description and interpretation of deep reflection patterns, which provide a new vision to study the pattern of continental hyperplasia and superimposed reconstruction at northern margin of North China Craton.

## **2. Geological tectonic setting**

The study area mainly involves two tectonic units, a suture zone and a large fault zone. The tectonic unit in the north is the Songliao-Xilinhote Massif, mainly composed of Phanerozoic metamorphic basement and a massive Mesozoic-Cenozoic sedimentary cover ([Zhang et al., 1998](#)). Some scholars also believe it was a composite basement of Paleozoic orogenic construction and Cambrian construction ([Zhang et al., 2008](#)). Especially in recent years, the ancient ages obtained successively in Xilingol area, about 300 km to the west of the study area, confirm the existence of the Precambrian basement, but the geotectonic units to which it belongs are still in great debate ([Xu et al., 2015](#); [Liu et al., 2017](#)). A complete upper Paleozoic sedimentary system was developed on the west side of the study area, indicating that the tectonic environment was relatively stable ([Wang et al., 2009](#)).

The North China Craton in the south is one of the oldest Precambrian cratons in the world, with the Bainaimiao island arc developed along its northern margin, which

extended from the north of Bayan Obo, through Bainaimiao, Tulingkai, Jiefangyingzi, to the south of Jilin (Zhao et al., 2010), and the arc proliferated to North China Craton by arc-land collision at the end of early Paleozoic. During early and middle Devonian, alkaline complexes of 410~380Ma developed in the northern margin of the NCC, which may be related to the extension events after arc-land collision. From the late Carboniferous, the northern margin of the North China Craton developed into the Andean active continental margin, it appeared as a passive rift zone and an alkaline rock zone during the Permian (Xu et al., 2015).

The boundary between the two tectonic units is the Xar Moron Suture, which has relatively complete ophiolite belts scattered through Kedanshan, Wudaishimen, Erbad, Xinshuwa and Jiujiangzi regions (Li et al., 1986). Among these ophiolites, the Jiujiangzi ophiolite is only 20 km away from deep seismic reflection profile in this paper. Zircon U-Pb dating results of the gabbro dyke and surrounding rocks of the ophiolite by Liu et al. (2016) show that the original rocks were formed in the late early Permian and the tectonic embeds were from the end of late Permian to the beginning of early Triassic.

Mesozoic magmatic rocks are widely developed in the study area, including Triassic granites, Cretaceous granites and volcanic rocks, etc. Li et al. (2007) conducted geochemical analysis of the syn-collisional granite intruding into the late Paleozoic collision complex in Shuangjingzi area, and believed that the rock was crust-originated, possibly from the accretion of Paleozoic and the recycling of the relatively old continental margin. Cretaceous granite is exposed in a large area in the southern Part of The Greater Hinggan Mountains to the northwest of the study area (Wu et al., 2011), and it is believed to be formed in the extensional environment after the Jurassic Paleo-Pacific subduction.

The Nenjiang-Balihan Fault is a large normal fault or detachment fault in lithospheric scale with left strike-slip characteristics (Han et al., 2012; Liu et al., 2011) that runs NNE through the study area. It separates the present Great Xing'an Mountain from the Songliao Basin to the east, and controlled the formation and evolution of the Mesozoic and Cenozoic fault depression basins. The southern part of this fault cut off the Xar Moron Suture, with an estimated displacement of 40-50km (Han et al., 2012).

### **3. Seismic data acquisition and processing**

The 160-km-long deep seismic reflection data was acquired in 2016, straightly extended northwest to southeast from Ar Horqin Banner, via Kailu and Ongniud Banner to Naiman Banner. It was acquired using the French SERCEL 428XL recording system with 24-bit digital geophones. To obtain high-resolution seismic images of the entire lithosphere, three types of explosive sources were employed with three charge sizes of 24 kg, 96 kg and 480 kg. The 24-kg shots were placed in single shot holes at a depth of 25 m with the 200-m spacing interval. The 96-kg shots were placed in a cluster of three shot holes at a depth of 30 m with 800 m spacing interval. The 480-kg shots were placed in clusters of 12 shot holes with 25-km spacing interval. 800 receiving traces were employed with geophone group spacing of 50 m to record, and the minimum and maximum shot-receiver offsets were 25 m. Recording was at a 2 ms sample interval for 50 s with 100-fold common mid-point coverage for the processing. The data acquisition parameters are listed in Table 1.

High fidelity and amplification-preservation processing flow is employed during data processing to enhance the effective signal from deep structures, as well as retain the signatures of shallow reflectors, which includes: (1) tomographic static correction is

used to eliminate the effects of rugged topography conditions upon the long-offset seismic data, and estimated the shallow chromatography velocity by topography inversion; (2) Multi-domain pre-stack noise suppression, such as f-x domain and f-k domain; (3) Spherical divergence compensation and geometric diffusion compensation are used to compensate the deep and large offset energy; (4) Surface consistent amplitude compensation and amplitude consistent deconvolution are used to solve the problems of distinct amplitude difference and inconsistent frequency range caused by different charge size of shots and distinctly differential surface excitation conditions; (5) The accuracy of velocity analysis under the condition of large offset is improved by high order velocity analysis, the residual static correction problem is solved by multiple iterations of residual static correction, and the quality of data is improved by using multi-focus imaging technology; (6) The anisotropic pre-stack time migration technique is used to obtain accurate migration imaging velocity and to accurately image complex structures. Detailed processing flow is list in table 2, a typical shot after data processing is shown in figure 3, and the final migrated profile is shown in figure 4b.

#### **4. Seismic reflections, patterns and discussion**

The carefully processed profile (fig. 4) presents the reflection characteristics of "longitudinal stratification and transverse partitioning", the reflection characteristics in the crust are clear, the Moho reflection is intermittent but traceable, and the reflections in the upper mantle of the lithosphere is obvious. According to different reflection characteristics transversely, the study area can be successively divided into the Songliao-Xilinhhot Massif, the connective zone and the northern margin of North

China Craton.

#### **4.1 Unified depth but different seismic patterns of Moho reflection**

The Moho reflection of the study area is weak, it is identified by a discontinuous interface in the range of 11-12s, which divided the lithosphere into the upper reflective area and the lower non-reflective area, it is considered to be the Moho reflection of the study area with approximate depth of 33-36 km. However, the seismic patterns of Moho differs along the profile, as follows: (1) the Moho reflection on both sides of the profile is obvious and the seismic pattern is relatively simple; (2) the connective region in the central (CDP, 2200-5800) has a more complex seismic pattern, which is composed of multiple sets of reflections, with many faults and overlaps, and cutting the dipping reflections extend from the crust to upper mantle. Within an overall compare, the depth of the Moho in the study area is approach to that of Northeast China and North China (Xu et al., 2017; Hou et al., 2015; Fu et al., 2019), we speculated that the Moho observed today is a modified Moho after a unified tectonic event, and the middle part of the survey line is obviously superimposed on the early structure.

#### **4.2 Lateral unified upper crust reflection**

The lateral subdivision of the upper crust is not very obvious. The middle and south part of the profile, corresponding to the southwest part of the Songliao Basin, show strong reflections at the top of crust, which represents sedimentary layers, and the seismic events gradually deepening to the southeast. According to the shallow velocity structure (fig. 4a), the sediments were as thick as 1500 m. The northwestern mountainous areas also show deposits of a certain thickness, which may correspond to some exposed upper Paleozoic strata or sediments filled in the strike-slip fault system.



There is an obvious blank reflection area under the shallow sedimentary layer with the depth of 1000 – 7000 m (2- 3 s, TWT), and its velocity is more than 5000 m/s. Few sedimentary rocks can reach this level under the condition of this buried depth. Combined with the exposed Jurassic volcanic rocks and cretaceous granite, it is inferred that this weak reflection zone may correspond to igneous rock reflection zone of granite or volcanic rock. The suspected igneous blank reflection zone is based on a discontinuous arc-shaped strong reflection zone (3-4 s, TWT, CDP, 2000-4000, 5200-6200, 7200-7800, etc.), which may be related to irregular interfaces formed by magma activities at different times.

#### **4.3 Lateral divided middle, lower crust and upper mantle reflections**

**Songliao-Xilinhote Massif (CDP, 6200-8293):** The middle and lower crustal reflections below 4s in this area are mainly weak reflections, except a reflection cluster composed of multiple short near-horizontal lens strong reflections (CDP, 7400-8000, TWT, 4-11s). This set of reflections has only a few kilometers transversely, but has the characteristic of high amplitude, corresponding to large wave impedance difference caused by obvious lithologic change. It only develops above the Moho, and may be related to the upward of multi-stage magma differentiation and crystallization. In addition, an near-horizontal reflection with good continuity and strong amplitude was observed at 7.5s, which was presumed to be the interfacial reflection of the middle and lower crust and may represent the tectonic slip surface. In this area, the upper mantle is nearly transparent below the Moho.,

**North margin of North China Craton (CDP, 597-2200):** The middle and lower crust of this area are also dominated by weak reflection, with only a small amount of near-horizontal reflection, mostly distributed in the lower crust. And interfacial

reflection of the middle and lower crust around 7.5s can also be observed. This area is connected to the central reflective area through a reflection cluster composed of multiple short near-horizontal strong reflections (CDP, 1800-2800, TWT, 4-10 s). However, this strong reflection cluster is different from the strong reflection cluster in the northwest (CDP, 7400-8000) as its contour has certain occurrence, which may indicates a magmatic structure superimposed on early structures. The top of the upper mantle in this region is also nearly transparent with some exception extended from the middle of the profile.

**The connective area (CDP, 2200-6200):** This area shows strong reflections, which are completely different from the both ends of the profile. It extends for more than 100 km laterally, and from 4s to 15s longitudinally. The structure of the middle crust is complex, including two sets of strong reflection areas with opposite tendencies, located in CDP 5400-5800 and 3500-3900 regions respectively, separated by small area weak reflection. The lower crust is mainly composed by a series of near-parallel south inclined reflections, which can be clearly observed on a pre-stack shot (Figure 3b), showing good continuity of high amplitude. Using an average crustal velocity of 6km/s, the apparent inclination of these near-parallel slant reflections is approximately 15-20°. Some of these tilted reflections can be traced to the mantle, so it may be formed earlier than the Moho reflection. The middle and lower crustal reflections at CDP 5800-6200 can form a group of "crocodile" tectonics, that is, a group of north-dipping middle crustal reflections and a group of south-dipping lower crustal reflections turn slightly and connect at the middle and lower crustal interface, showing a "spreading" pattern from north to south.

## 5. Discussion

### 5.1 Patterns of early Paleozoic - Early Mesozoic subduction

The most distinguished feature on Ar Horqin-Naiman profile is the strong inclined reflections in middle, lower crust and top of mantle beneath the Xar Mron Suture, which is the key to interpret the geotectonic features of the study area. But the interpretation of middle and lower crust and upper mantle reflection in different geotectonic environments is diverse, suggestions for reflective middle and lower crust have included: (1) tectonic underplating of continental crust by fragmented oceanic lithosphere (Green et al. 1986) or thick oceanic sedimentary sequences (Moore et al., 1991); (2) seismic lamination and anisotropy caused by ductile deformation in the warm and low-viscosity lower crust (Meissner, 2006), (3) mafic/ultramafic intrusions of partial melts derived from the upper mantle (Singh and Mckenzie, 1993). The former usually formed at convergent area while the latter two are usually found in extensional tectonic area and are mostly near horizontal reflection.

The mantle reflections can be divided into four categories by Steer (1998): (1) distinct dipping events that appear to originate in the lower crust and continue some distance into the upper mantle; (2) discontinuous, diffusely distributed, or isolated reflections at varying depths; (3) sub-horizontal reflections tens of kilometers in extent, often interpreted as the 'base of the lithosphere'; (4) very deep reflections in the mantle lithosphere. The mantle reflections observed in this study can be seen as belonging to the first category, which is most observed mantle reflection on deep seismic profiles around the world (Smythe et al., 1982; van der Velden, 2005), especially beneath continental margins and ancient sutures.

Combined with previous studies on ophiolite and granite outcrops in the west of the

study area, it is believed that these remarkable reflections represented the subduction deformation structure of the Paleo Asian Ocean, and had the following characteristics:

(1) The leading edge of the subduction zone shows consistent southern dipping reflections at the range of CDP 2200-4800, TWT 5-14s, which were superimposed by the intermittent Moho reflection. We consider it to be similar to the reflection characteristics of oceanic sediments or oceanic lithosphere overlying through a series of faults or ductile zones caused by oceanic subduction around the world, like the west coast of North America (Cook et al., 2010).

(2) The back side of the subduction zone shows obvious "crocodile" tectonics reflection characteristics in the range of CDP 4800-7000, TWT 5-14s, which is very similar to many continental collision structures around the world, such as, the Variscan mountain belts in Europe, the Alpides, Laramide orogenic in North America (DEKORP Research Group et al., 1990; Brown et al., 1986). We suggest it to be the product of the decoupling deformation of the middle and lower crust of the Songliao - Xilinhote massif during the continental collision. It had a relatively small scale as the upper part of the "crocodile" tectonics structure didn't cover the front dipping reflections. It was accorded with the characteristics of "soft collision orogeny" in NE China.

So, the range of tectonic deformation caused continental fitting can be determined within the CDP 2200 to 6200. Consider the Mesozoic Nenjiang-Balihan fault, which caused about 40-50km left-lateral strike-slip in this area, as well as the general trend of suture zone determined by predecessors, the range of subduction deformation of the suture is given as shown in fig. 2, the estimated width of the suture zone is about 100 km, and subduction polarity in this area is southward. It is worth mentioning that

within the range of 5600 to 6600 CDP, some weak southern dipping mantle reflections can be recognized near the Moho, which may be a reflection of the slight reverse deformation in the continental collision stage, but don't mean there is any obvious bidirectional subduction patten. This may indicate that the northern end of the subducted branch ocean was always a passive continental margin until the final continental collision, but the profile length was limited, and the discussion on this issue should be combined with more data.

## **5.2 Reflections from Mesozoic magmatic activity and regional extension**

A series of magmatic structures Such as Triassic granite, Jurassic volcanic rocks and Cretaceous granite can be observed superimposed on subduction structures in Ar Horqin-Naiman profile:

(1) Two clump-like weak reflection areas, in addition to the inclined strong reflection structure can be found in the middle crust of the sutured zone, which are formed superimposed on the early subduction structure, and are presumed to be granite intrusion in the period of syn-collision and post-collision.

(2) Weak reflection zone can be observed at range of 1-3s (TWT) covering the early Triassic collision. Combined with the large amount of Jurassic volcanic rocks exposed and its higher velocity, it is considered to these volcanic rocks. Meanwhile, the strong reflection clusters connecting the weak reflection zone and the middle and lower crust may also be the product of volcanic activities in this period, and the formation reason may be the upwelling of heat flow diapir formed the wave formation resistance interface with multiple penetrations through multiple differentiation and crystallization under the background of extensional structure.

(3) mid-crustal blank reflections at the edge of the Songliao - Xilinhote Massif in this

section is speculate to the Cretaceous granite as it massive crops out in the Great Xing'an Mountains area to the northwest of the study area (Wu et al., 2011).

In addition to the magmatic activity, Mesozoic extensional are also manifested by shallow fault depression and large strike-slip or normal faults. Combined with the results of shallow strong reflection and tomographic velocity of the profile, it can be seen that several small fault depressions corresponding to the fault depression period in the Songliao Basin of early Cretaceous (Wang et al., 2016). And the Moho may be renewed at this period. There are also small-scale sedimentary strata on the west side of the study area, which may be the sediments filling the secondary fault zone of Nenjiang-Balihan strike-slip fault. And we speculate that the Nenjiang-Balihan fault, as the boundary fault of Songliao basin, developed along the weak zone of early structure in the process of cutting the Xar Moron Suture, so it could not be clearly identified at the study area.

### 5.3 Structural evolution of the study area in phanerozoic

During early Paleozoic to late Cretaceous, the study area underwent the superimposed reconstruction of the closure of the Paleo-Asian Ocean and the subduction of Paleo-Pacific Ocean, which caused some structure preserved in the lithosphere, we divided into the following three stages:

**(1) Oceanic subduction (Ordovician to the end of Permian):** According to the exposed ophiolite and igneous rocks related to the oceanic crust material remelting regeneration in the west of study area, we suggest that some superposition and deformation of oceanic lithosphere and sediments through a series of faults or ductile zones may occurred during oceanic subduction. However, according to the principle

of equal volume, even if the subduction zone delineated in fig. 5 is full of piled oceanic crust, the amount of oceanic crust it represents is limited and insufficient to represent a branching ocean. Therefore, the oceanic crust of the branching ocean is still subducted into the deeper part of the mantle at a certain stage, instead of only accumulating in the northern margin of the North China Craton. During this stage, the alkaline rock zone is developed in the back side of the subduction zone under the action of tensile stress.

**(2) Continental collision (Early Triassic):** The integration of the Songliao-Xilinhote massif and the North China Craton entered the final stage in this period. The oceanic lithosphere, which was originally emplaced between the two blocks, subducted under the North China Craton in large quantities, but some of them piled up in the northern margin of the North China Craton. Meanwhile, the middle and lower crust of the Songliao-Xilinhote massif was decoupled, and the middle and upper crust thrust upward, pushing the relict oceanic crust accumulated in the leading edge out of the surface. The lower crust was subducted and stopped under the action of inertia. During this period, the crust was significantly thickened and a large amount of syn-collision granite developed.

**(3) Post-orogenic extension and reconstruction (Late Triassic to Cretaceous):** a large area of late Triassic and Jurassic volcanic rocks were exposed in the study area. We speculated that during this period, the study area experienced a post-orogenic extension, during which the crust began to thin and the oceanic lithosphere material accumulated in the northern margin of the North China Craton reworked under the action of upwelling heat. The blank reflection of volcanic rock on Ar Horqin-Naiman Profile is the product of this period, as well as the strong reflection in clusters representing upwelling of deep materials. In the Cretaceous, the Paleo-Pacific

tectonics significantly affected the region, which was mainly reflected in the development of large area of Cretaceous granite and the Nenjiang-Balihan fault. Meanwhile, southeast side of study area entered its basin evolution stage, and a large number of extensional tectonics were developed to receive deposition.

## **6 Conclusions**

This paper describes and analyzes the reflection characteristics of the deep seismic reflection profile from Naiman to Ar Horqin Banner, the following conclusions are drawn:

(1) The study area presents the reflection characteristics of "longitudinal stratification and transverse partitioning". In the middle, lower crust and upper mantle of the profile, the reflection is mainly southward inclined, which is completely different from the weak reflection and a small amount of near-horizontal reflection on both sides, which suggests that the Solonker-Xar Moron-Changchun-Yanji Suture extended though the area of Ar Horqin Banner to Naiman Banner. The width of the suture was about 100km, and its subduction polarity was southward.

(2) Two stages of the closure of the Paleo-Asian Ocean in the study area are divided, namely the stage of oceanic subduction and continental collision. The former is recognized by a large area of south dipping reflections, and the latter is featured by a set of "crocodile-like reflection", but it had a relatively small scale, which was accorded with the characteristics of "soft collision orogeny" in NE China.

(3) Magmatic activities related to continental fitting are identified, which are, deep intrusive rocks represented by large area of blank reflection in the crust of the North China Craton during the early oceanic subduction, two blank reflection zones in the



reflective zone beneath the suture zone developed at the post- collision stage, and the volcanic rocks and magma channel, represented by the weak reflection zone around 1~3s (TWT), as well as strong reflection clusters.

## **Acknowledgments**

We are grateful to Professor An Yin for his very helpful and constructive advises. This work was jointly supported by China Geological Survey (Grant no. DD20160207, DD20190010), Natural Science Foundation of China (Grant nos. 41474081, 41590863) and National Key Research and Development Program of China (2107YFC0601301). More typical shots from different tectonic units and the final stacked profile are available in the supporting information of this paper. The raw deep seismic data and guidance on data sharing are available on the website of SinoProbe Center: <http://www.sinoprobe.org/shuju.aspx?page=gongxiang>, and the data management center of SinoProbe: <http://124.17.88.221/sinoprobe/>.

## **References**

- Brown, L.D., Barazangi, M., Kaufman, S. (1986). The first decade of COCORP: 1974-1984. // Barazangi, M., Brown, L. D., eds. Reflection seismology: A global perspective. Am geophys. Union, Geodyn. Ser., 13, 107-120.
- Cook, F.A., Spence, G., White, D.J., Jones, A.G., Eaton, D.W.S., Hall, J., Clowes, R.M. (2010). How the crust meets the mantle: Lithoprobe perspectives on the Mohorovičić discontinuity and crust–mantle transition This article is one of a series of papers published in this Special Issue on the theme Lithoprobe — parameters, processes, and the evolution of a continent. Canadian Journal of Earth Sciences, 47, 315-351.
- DEKORP Research Group, Meissner, R., Wever, T.H., Sadowiak, P. (1990). Reflectivity patterns

in the Variscan mountain belts and adjacent areas: an attempt for a pattern recognition and correlation to tectonic units. *Tectonophysics*, 193, 361-378.

Eizenhöfer, P. R., Zhao, G., Zhang, J., and Sun, M. (2014), Final closure of the Paleo-Asian Ocean along the Solonker Suture Zone: Constraints from geochronological and geochemical data of Permian volcanic and sedimentary rocks, *Tectonics*, 33, 441-463, doi:10.1002/2013TC003357

Eizenhöfer, P.R., Zhao, G. (2018). Solonker Suture in East Asia and its bearing on the final closure of the eastern segment of the Palaeo-Asian Ocean. *Earth-Science Reviews* 186, 153-172.

Fu, W., Hou, H.S., Gao, R., Liu, C., Yang, J., Guo, R. (2019). Fine structure of the lithosphere beneath the Well SK-2 and its adjacent: Revealed by deep seismic reflection profile. *Chinese Journal of Geophysics*, 2019, 1349-1361.

Gao, R., Lu, Z.W., Simon, L.K., Wang, H.Y., Dong, S.W., Li, W.H., Li, H.Q. (2016). Crust-scale duplexing beneath the Yarlung Zangbo suture in the western Himalaya. *Nature Geoscience*, 9, 1-7.

Green, A.G., Clowes, R.M., Yorath, C.J., Spencer, C., Kanasewich, E.R., Brandon, M.T., Brown, A.S. (1986). Seismic reflection imaging of the subducting Juan de Fuca plate. *Nature*, 319, 210-213.

Han, G., Liu, Y., Neubauer, F., Genser, J., Zou, Y., Li, W., Liang, C. (2012). Characteristics, timing, and offsets of the middle-southern segment of the western boundary strike-slip fault of the Songliao Basin in Northeast China. *Science China Earth Sciences* 55, 464-475.

Hou, H., Wang, H., Gao, R., Li, Q., Li, H., Xiong, X., Li, W., Tong, Y. (2015). Fine crustal structure and deformation beneath the Great Xing'an Ranges, CAOB: Revealed by deep seismic reflection profile[J]. *Journal of Asian Earth Sciences*, 113, 491-500.

Jian, P., Liu, D., Kröner, A., Windley, B.F., Shi, Y., Zhang, F., Shi, G., Miao, L., Zhang, W., Zhang, Q., Zhang, L., Ren, J. (2008). Time scale of an early to mid-Paleozoic orogenic cycle of the long-lived Central Asian Orogenic Belt, Inner Mongolia of China: Implications for continental growth. *Lithos*, 101, 233-259.

Li, J.Y. (1986). A preliminary study on the ancient suture zone between the Sino-Korean and Siberian plates in eastern Inner Mongolia. *Chinese Science Bulletin*, 14, 1093-1096.

444 Li, J.Y., Gao, L.M., Sun, G.H., Li, Y.P., Wang, Y.B. (2007). Shuangjingzi middle Triassic  
 445 syn-collisional crust-derived granite in the east Inner Mongolia and its constraint on the  
 446 timing of collision between Siberian and Sino-Korean paleo-plates. *Acta Petrologica Sinica*,  
 447 24, 565-582.

448 Li, S., Chung, S.L., Wilde S. A., Jahn B.M., Xiao W.J., Wang T., Guo, Q.Q. (2017). Early-Middle  
 449 Triassic high Sr/Ygranitoids in the southern Central Asian Orogenic Belt: Implications for  
 450 ocean closure in accretionary orogens, *J. Geophys. Res. Solid Earth*, 122.

451 Liu, C., Yang, B.J., Wang, Z.G., Wang, D., Feng, X., Lu, Q., Liu, Y., Wang, S.Y. (2011). The deep  
 452 structure of the western boundary belt of the Songliao Basin: the geoelectric evidence.  
 453 *Chinese Journal of Geophysics*, 54, 401-406. (in Chinese with English abstract).

454 Liu, J.F., Li, J.Y., Sun L.X., Yin, D.F, Zheng, P.X. (2016). Zircon U-Pb dating of the Jiujingzi  
 455 ophiolite in Bairin Left Banner, Inner Mongolia: Constraints on the formation and evolution  
 456 of the Xar Moron River suture zone. *Geology in China*, 43: 1947-1962(in Chinese with  
 457 English abstract).

458 Liu, Y.J., Li, W.M., Feng, Z.Q., Wen, Q.B., Neubauer, F., Liang, C.Y. (2017). A review of the  
 459 Paleozoic tectonics in the eastern part of Central Asian Orogenic Belt. *Gondwana Research*,  
 460 43, 123-148.

461 Liu, Y.J., Feng, Z.Q., Jiang, L.W., Jin, W., Li, W.M., Guan, Q.B., Wen, Q.B., Liang, C.Y., 2019.  
 462 Ophiolite in the eastern Central Asian Orogenic Belt, NE China. *Acta Petrologica Sinica* 35:  
 463 3017-3047.

464 Meissner, R., Rabbel, W., Kern, H. (2006). Seismic lamination and anisotropy of the Lower  
 465 Continental Crust. *Tectonophysics*, 416, 81-99.

466 Moore, J.C., Diebold, J., Fisher, M.A., Sample, J., Brocher, T., Talwani, M., Ewing, J., Huene, R.v.,  
 467 Rowe, C., Stone, D., Stevens, C., Sawyer, D. (1991). EDGE deep seismic reflection transect  
 468 of the eastern Aleutian arc-trench layered lower crust reveals underplating and continental  
 469 growth. *Geology*, 19, 420.

470 Pei, F., Xu, W., Yang, D., Zhao, Q., Liu, X., Hu, Z. (2007). Zircon U-Pb geochronology of  
 471 basement metamorphic rocks in the Songliao Basin. *Chinese Science Bulletin*, 52, 942-948.

472 Sengör A M C, Natal'in B A. Paleotectonics of Asia: Fragments of a syn thesis. 1996. // Yin A,

473 Harrison M eds. The Tectonic Evolution of Asia. Cambridge: Cambridge University Press.  
 474 Singh, S.C., McKenzie, D., 1993. Layering in the lower crust. *Geophys. J. Int.*, 113, 622-628.  
 475 Smythe, D.K., Dobinson, A., Mcquillin, R., Brewer, J.A., Matthews, D.H., Blundell, D.J., Kelk, B.  
 476 (1982). Deep structure of the Scottish Caledonides revealed by the MOIST reflection profile.  
 477 *Nature*, 299, 338-340.  
 478 Steer, D.N., Knapp, J.H., Brown, L.D. (1998). Super-deep reflection profiling: exploring the  
 479 continental mantle lid. *Tectonophysics*, 286, 111-121.  
 480 van der Velden, A.J. (2005). Relict subduction zones in Canada. *Journal of Geophysical Research*,  
 481 110, B08403.  
 482 Wang, C.W., Sun, Y.W., Li, N., Zhao, G.W., Ma, X.Q. (2009). Geotectonic significance of late  
 483 Paleozoic stratigraphic distribution in northeast China and adjacent areas. *Science China*  
 484 *Earth Sciences*, 39, 1429-1437. (in Chinese).  
 485 Wang, P.J., Mattern, F., Didenko, N.A., Zhu, D.F., Singer, B., Sun, X.-M. (2016). Tectonics and  
 486 cycle system of the Cretaceous Songliao Basin: An inverted active continental margin basin.  
 487 *Earth-Science Reviews*, 159, 82-102.  
 488 Wang T, Guo L, Zhang L, et al. (2015). Timing and evolution of Jurassic–Cretaceous granitoid  
 489 magmatisms in the Mongol–Okhotsk belt and adjacent areas, NE Asia: Implications for  
 490 transition from contractional crustal thickening to extensional thinning and geodynamic  
 491 settings. *Journal of Asian Earth Sciences*, 97(Part B, 1):365-392.  
 492 Wilde, S.A. (2015). Final amalgamation of the Central Asian Orogenic Belt in NE China:  
 493 Paleo-Asian Ocean closure versus Paleo-Pacific plate subduction — A review of the evidence.  
 494 *Tectonophysics* , 662, 345-362.  
 495 Wu, F.Y., Sun, D.Y., Ge, W.C., Zhang, Y.B., Grant, M.L., Wilde, S.A., Jahn, B.M. (2011).  
 496 Geochronology of the Phanerozoic granitoids in northeastern China. *Journal of Asian Earth*  
 497 *Sciences*, 41, 1-30.  
 498 Xiao, W., Windley, B.F., Hao, J., Zhai, M. (2003). Accretion leading to collision and the Permian  
 499 Solonker suture, Inner Mongolia, China: Termination of the central Asian orogenic belt.  
 500 *Tectonics* ,22, n/a-n/a.

- Xu, B., Zhao, P., Wang, Y., Liao, W., Luo, Z., Bao, Q., Zhou, Y. (2015). The pre-Devonian tectonic framework of Xing'an–Mongolia orogenic belt (XMOB) in north China. *Journal of Asian Earth Sciences*, 97, 183-196.
- Xu, M., Li, Y.L., Hou, H.S., Wang, C.S., Gao, R., Wang, H.Y., Han, Z.P., Zhou, A. (2017). Structural characteristics of the Yilan–Yitong and Dunhua–Mishan faults as northern extensions of the Tancheng–Lujiang Fault Zone: New deep seismic reflection results. *Tectonophysics*, 706-707, 35-45.
- Yuan, Y.Z., Zhang, X.B., Zhang, P.H., Zhong, Q. (2015). An analysis of gravity magnetic and electric characteristics of the Xar Moron River fault. *Geophysical and Geochemical Exploration*, 39, 1299-1304. (in Chinese with English abstract).
- Zhang, F.Q., Chen, H.L., Dong, C.W., Yu, X., Xiao, J., Pang, X.M., Cao, R.C., Zhu, D.F. (2008). Evidence for the existence of Precambrian Basement under the northern Songliao basin. *China Geology*, 35, 421-428. (in Chinese with English abstract).
- Zhang, M.S., Peng, X.D., Sun, X.M. (1998). The Paleozoic tectonic geographical pattern of northeast China. *Liaoning Geology*, 91-96. (in Chinese with English abstract).
- Zhang, S. H., Gao, R., Li, H. Q., Hou, H. S., Wu, H. C., Li, Q., Yang, K., Li, C., Li, W. H., Zhang, J. S., Yang, T. S., Keller, G.R. and Liu, M. (2014), Crustal structures revealed from a deep seismic reflection profile across the Solonker suture zone of the Central Asian Orogenic Belt, northern China: An integrated interpretation: *Tectonophysics*, 612-613, 26-39.
- Zhang, X.Z., Guo, Y., Zeng, Z., Fu, Q., Pu, J.B. (2015.) Dynamic evolution of the Mesozoic-Cenozoic basin in the northeastern China. *Earth Science Frontier*, 22, 88-98.
- Zhao, Y., Chen, B., Zhang, S.H., Liu, J.P., Hu, J.M., Liu, J., Pei, J.L. (2010). Pre-Yanshanian geological events in the northern margin of the North China Craton and its adjacent areas. *China Geology*, 37, 900-915.
- Zhou, J.B., Wilde, S.A., Zhao, G.-C., Han, J. (2018). Nature and assembly of microcontinental blocks within the Paleo-Asian Ocean. *Earth-Science Reviews*, 186, 76-93.

528 **Table 1 Data acquisition parameters of seismic reflection data**

Content	Parameter
Recording system	428XL
Gain	12 dB
Low cut	OUT
High cut	250 Hz
receiving traces	800
Geophone type	20-DX (10Hz)
Geophones/group	Linear combination for a string of 12 Geophones
recording format	SEG-D
Recording length	50 s
Sample rate	2 ms
Trace spacing	50 m
Minimum offset	25 m
Maximum offset	19975 m
Arrangement	19975-25-50-25-19975
Coverage	100-fold
Source type	Explosives
charge size	24 kg, 96 kg, 480 kg
Shot point interval	200 m (for 24-kg shot), 1000 m (for 96-kg shot)、 25km (for 480-kg shot)
Shot depth	25 m 30 m×3 (for 96-kg shot), 30 m×12 (for 480-kg shot)

529

530

531

532

533

534     **Table 2 Processing steps of seismic reflection data**

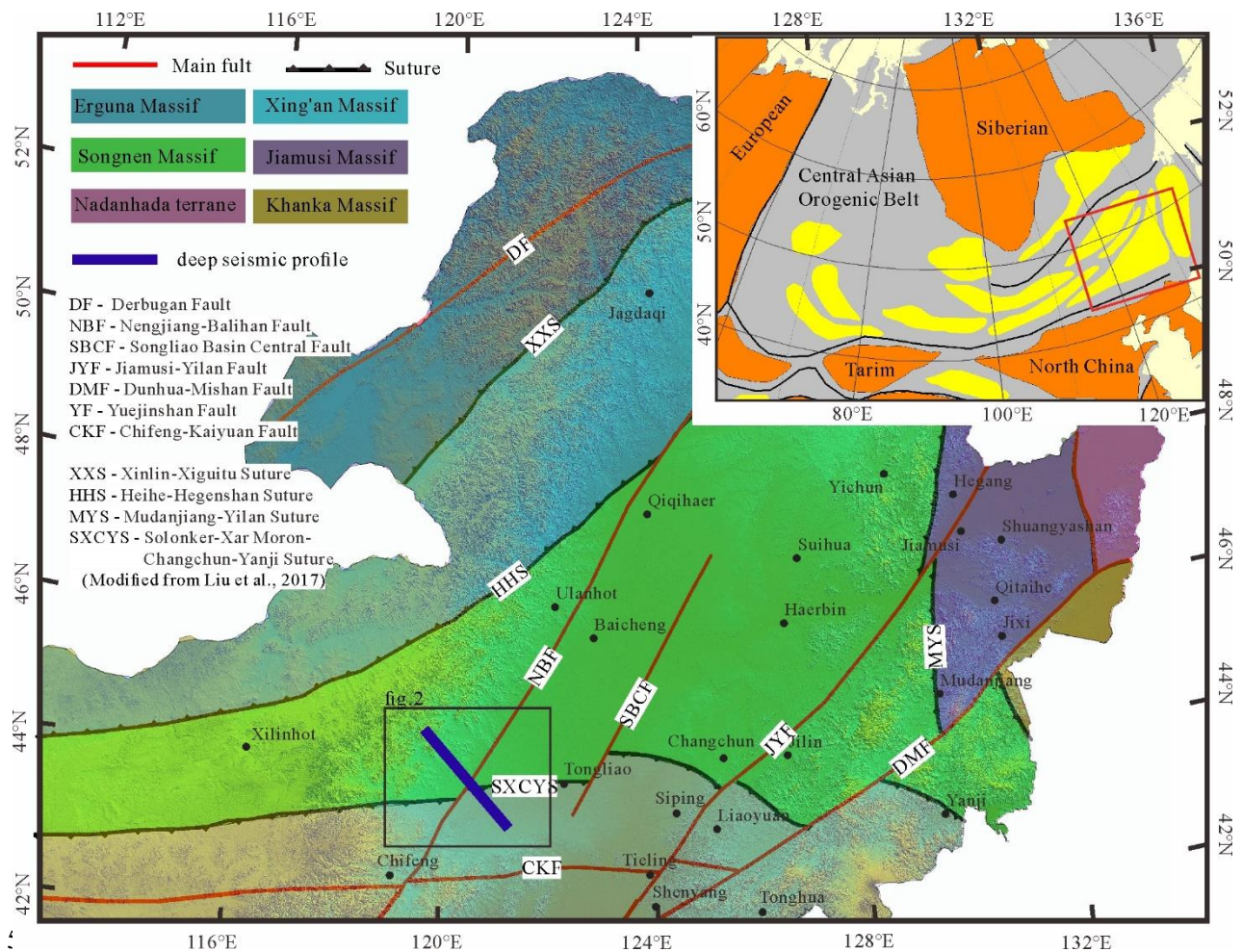
---

SEG-D input
2D line geometry definition, 25 m binning distance
Trace edition, trace length 30s, sample rate 4 ms
Band-pass filter, 6-10-44-50 (shallow) 、 2-4-24-30 (deep)
First breaks picking with full offset range
Tomographic statics correction, replacement velocity 2000km/s, final datum 1000 m
Combined spherical divergence and surface consistent amplitude correction
Stack multi-domain (t-x, f-k) de-noise
Surface consistent predictive deconvolution, operator length 200 ms, gap 12 ms, white noise 0.5%
Velocity analysis, 40 CMP
Surface consistent residual statics correction, 5 times (iteratively to velocity analysis)
High-order NMO correction, Manual mute
Multi - focus imaging
Pre-stack time migration, Kirchhoff summation, migration aperture 10000, migration angle 45°
Stack and post-stack filter

---

535

536



538 Fig.1 Tectonic division of the NE China and the location of Naiman - Ar Horqin  
539 Banner deep seismic profile. The tectonic map is simplified from Liu et al., 2017.



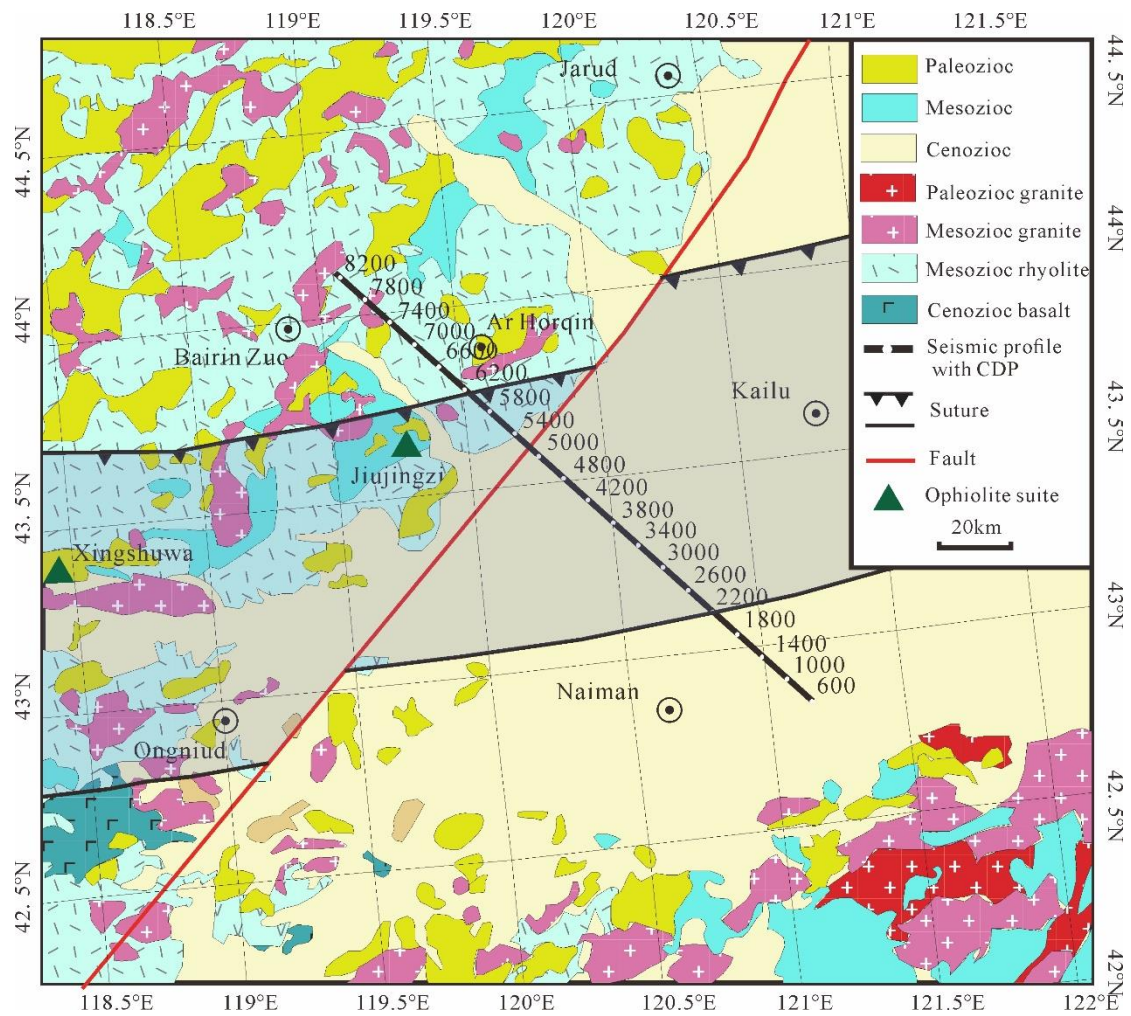


Fig.2 Location of the Naiman - Ar Horqin deep seismic profile on simplified geological map

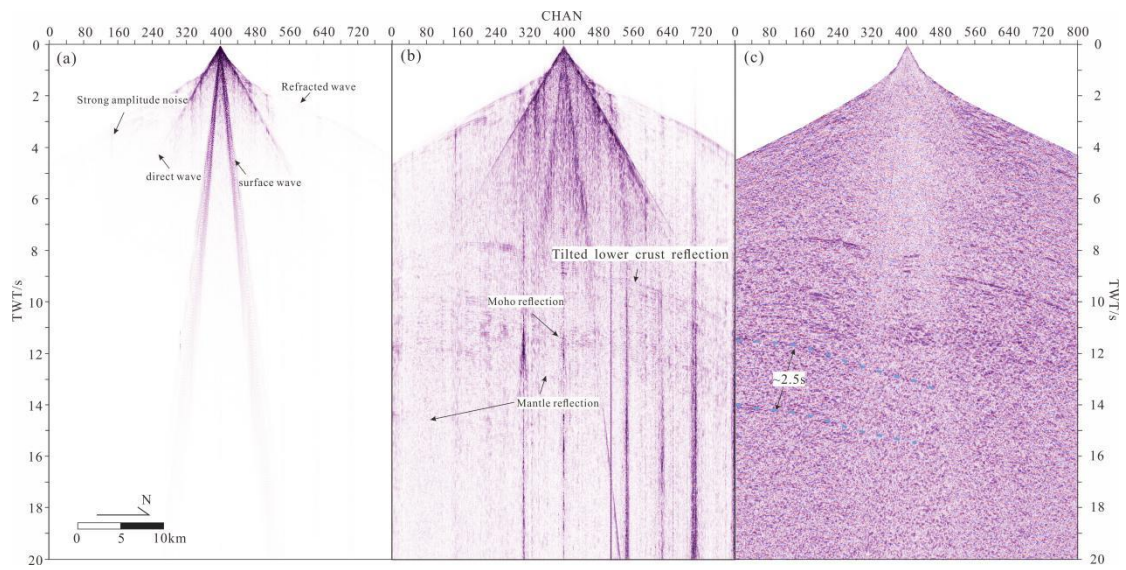
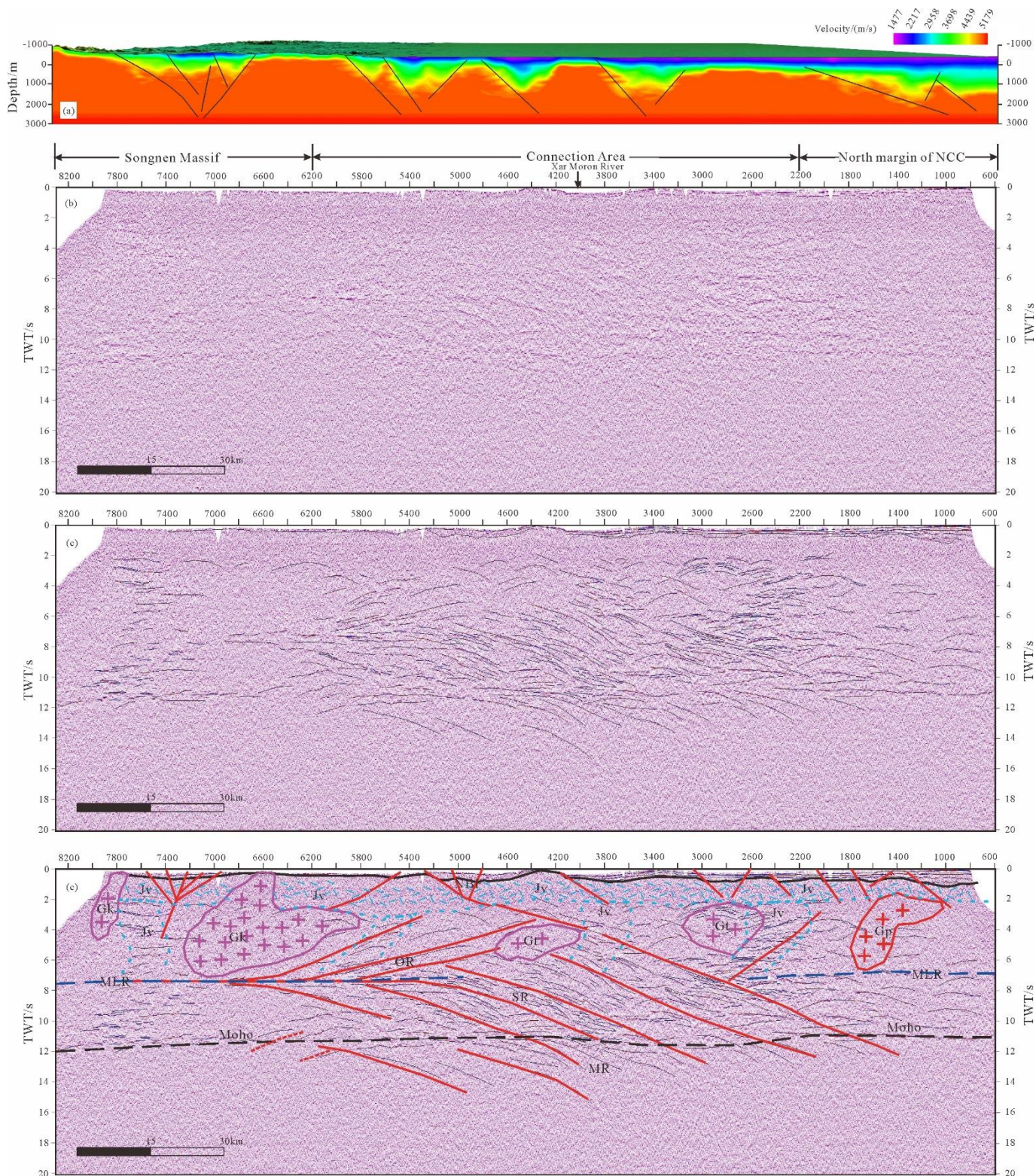


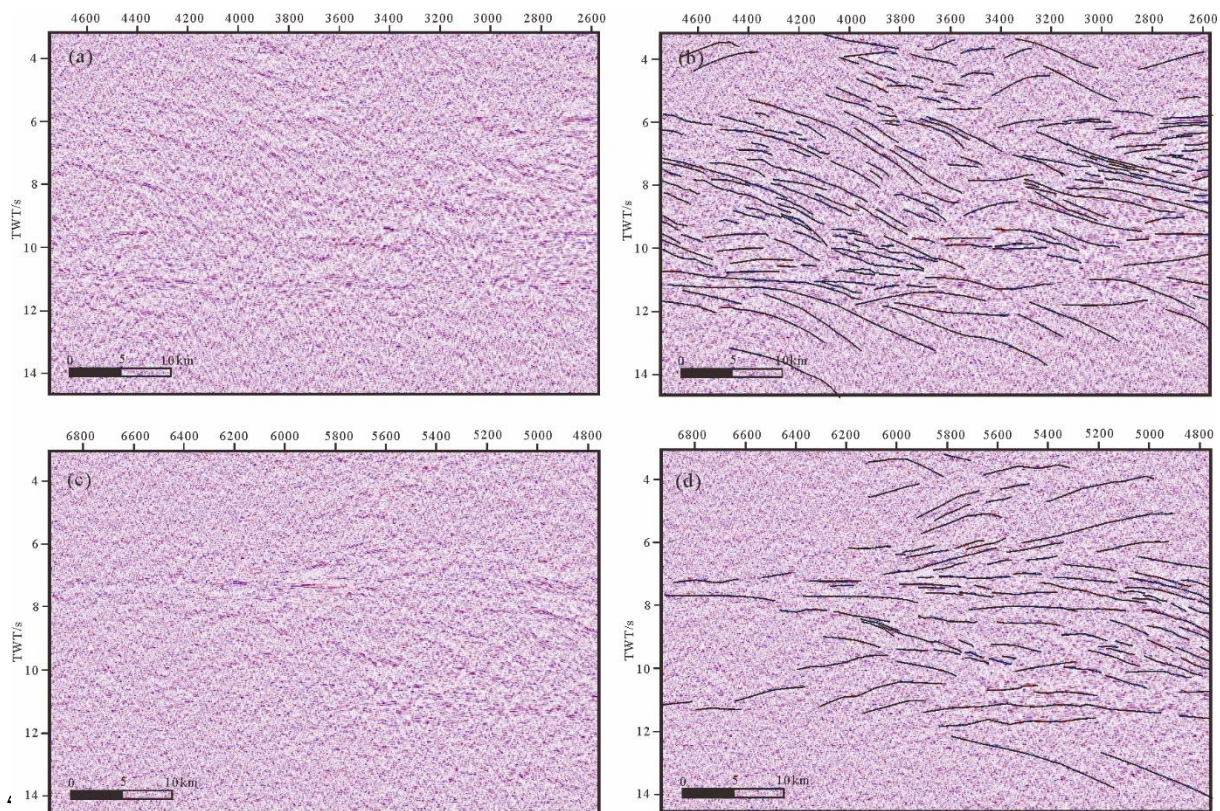
Fig.3 Typical shot beneath Xar Moron Suture: (a) original shot, (b) shot after less data processing (bandpass filter: 8-10-40-50, display with Fixed amplitude gain), (c) the record after precise data processing





551 Fig.4 Deep seismic reflection profile from Naiman to Ar Horqin Banner: (a)  
 552 topography and surface layer velocity profile acquired by tomographic inversion; (b)  
 553 pre-time migration profile; (c) profile with line drawing of the main reflections; (d)  
 554 Interpretation of the profile





556

557 Fig. 5 The deformed middle and lower crust and mantle beneath the connective area  
 558 of the Songliao - Xilinhote Massif the North China Craton

559 Fig. 5(a) and (b) show consistent southern dip reflections at the leading edge of the  
 560 subduction zone; Fig. 5(c) and (d) show "crocodile" tectonic reflection at back side of  
 561 the subduction zone

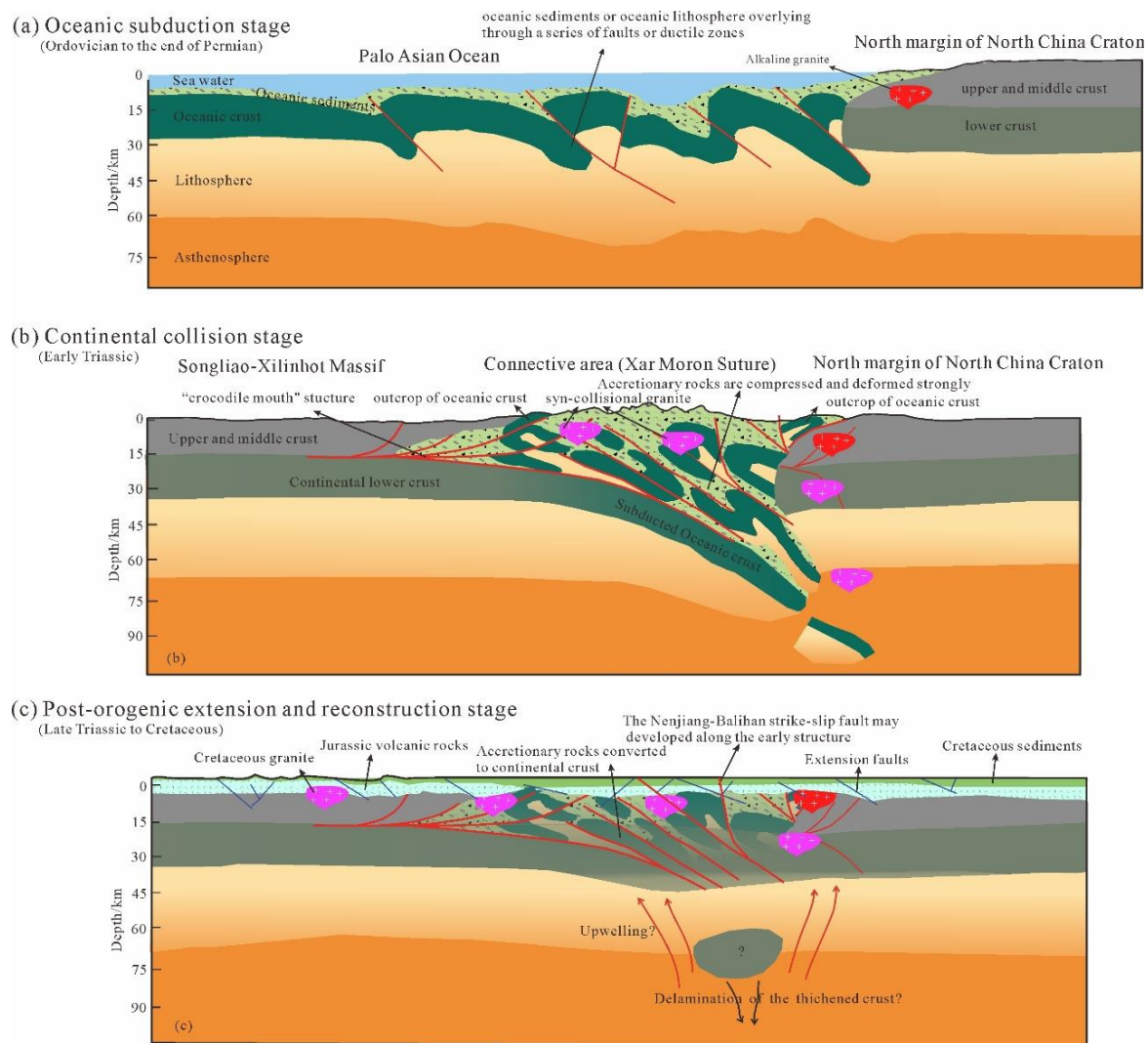


Fig.6 Structural evolution of the study area in phanerozoic: (a) Oceanic subduction; (b) Continental collision; (c) Post-orogenic extension and reconstruction by Paleo-Pacific domain